The Characterization of Organic Monolayers by FTIR External Reflectance Spectroscopy

Ultrathin organic films, which range in thickness from <1 nm to a few nanometers, can substantially alter the electronic, photonic, and structural properties of materials. In this article, we describe a class of molecules that dramatically affects the characteristics of gold surfaces by spontaneously forming ordered monolayers and discuss how Fourier transform–infrared–external reflectance spectroscopy (FTIR-ERS) can be used to characterize such surfaces. The introduction focuses on background and some key instrumental aspects of FTIR-ERS, followed by a discussion of three recent applications of FTIR-ERS to organomercaptan monolayer chemistry.

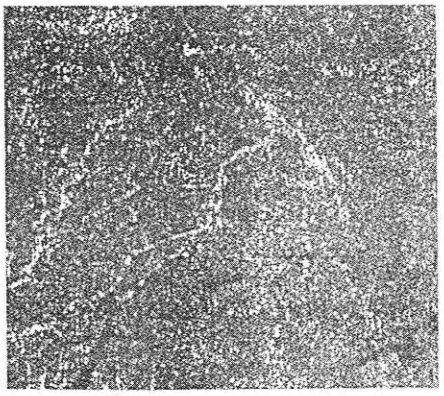

Richard M. Crooks* **and Chuanjing Xu**
Texas A&M University, Department of Chemistry, College Station, TX 77843-3255
Li Sun
University of Minnesota, Minneapolis
Stephen L. Hill*
Bio-Rad Digilab, 237 Putnam Avenue, Cambridge, MA 02139
Antonio J. Ricco*
Microsensor Department 1315, Sandia National Laboratories, P.O. Box 5800, Albuquerque, NM 87185
*Authors to whom correspondence should be addressed.

Because nanometer-scale coatings can dramatically alter the electronic, photonic, and structural properties of materials, it is becoming increasingly important to develop analytical methods for their characterization (1–3). The first techniques developed for characterizing ultrathin coatings were ultrahigh-vacuum electron spectroscopies such as x-ray photoelectron spectroscopy (XPS), Auger electron spectroscopy (AES), and low-energy electron diffraction (LEED). These methods, however, are costly to implement, typically provide limited molecular information, and often damage organic surfaces.

Increasingly, reflection infrared spectroscopic techniques are used for surface characterization because they provide highly detailed information about molecular structure and intermolecular interactions, are nondestructive, and are relatively easy to implement. The two families of surface-infrared techniques are Fourier tranform–infrared–internal reflection spectroscopy (FTIR-IRS) (4–6), which often uses multiple reflections to increase the spectroscopic signal-to-noise ratio (S/N), and FTIR–external reflection spectroscopy (FTIR-ERS), which usually involves a single reflection. The single-reflection FTIR-ERS approach is somewhat more versatile than the FTIR-IRS technique because any flat, reflective surface can be used as the substrate. However, the FTIR-ERS method usually results in a significantly lower S/N than FTIR-IRS.

This article focuses on FTIR-ERS, emphasizing the technique's application to the characterization of structurally ordered organic monolayers confined to metallic surfaces. Such monolayers are good models for studying adhesion (7), lubrication (8), wetting (9), and interfacial electron transfer (10), and they are now finding technological uses as ultrathin lithographic resists and chemical sensing elements (11–14).

BACKGROUND

FTIR-ERS of thin organic films confined to metal substrates is sensitive to the polarization and incident angle of the IR radiation as well as the orientation of the electric dipoles associated with the films. Light polarized with its electric vector parallel to the surface (*s*-polarized) results in a low-intensity electric field at the film–metal interface at all incident angles, because the electric-field dipole and its image dipole are antiparallel and of equal magnitude; that is, they sum to zero field strength (Figure 1a). This situation prevents absorption of *s*-polarized radiation by a surface-confined vibrating dipole (15,16).

In contrast, *p*-polarized light, which has its electric-field vector polarized perpendicular to both the *s*-polarized electric-field vector and the direction of propagation of the incident light, has a nonzero electric-field vector component perpendicular to the surface (Figure 1a). This component is maximized at Brewster's angle (ϕ), which is given by Equation 1:

$$\sin\phi \tan\phi = \frac{\sqrt{2}}{1.05 \times 10^{-6} (\nu\varepsilon\rho)^{1/2}} \qquad [1]$$

where ν is the frequency of light, ε is the dielectric constant of the ambient phase, and ρ is the resistivity of the metal (17). For high conductivity metals such as aluminum, silver, gold, copper, and platinum, the Brewster's angles are >89.5° (17). This means that optimum spectral sensitivity is achieved at large angles of incidence with *p*-polarized light. At present, angles in the range of 87°–88° from the surface normal are the highest that can practically be achieved without a significant loss of radiant energy, and angles less than ~85° are most often used. For a more detailed account of the theoretical aspects of FTIR-ERS, see the excellent review by Porter (18).

The surface-infrared selection rule states that only vibrating dipoles with a nonzero component perpendicular to the substrate surface will be excited by *p*-polarized infrared radiation (Figure 1b) (16,18). This is an important advantage of FTIR-ERS over other surface spectroscopic techniques because it

provides a means for determining the average orientation of surface-confined molecules (3).

Because the number of molecules in a surface monolayer is small, absorption of light by molecules in the ambient phase may interfere with spectroscopic measurements. However, this difficulty can be easily overcome. For example, polarization modulation methods can be used to spectroscopically isolate and amplify the relatively weak absorption that results from surface-confined molecules (19). Our measurements are performed in an IR-transparent N_2 atmosphere. This approach normally limits FTIR-ERS to ex-situ measurements, but if the surface-confined species give rise to unique spectral bands, these absorptions can be used to monitor surface processes even in the presence of an absorbing ambient phase.

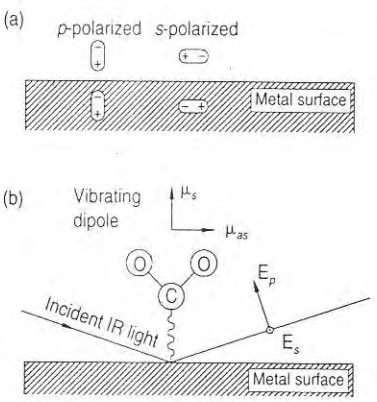

Figure 1. Schematic of the IR surface-selection rule. **(a)** The incident electric-field dipole and its image dipole cancel if the incident light is *s*-polarized (electric-field dipole parallel to the metal surface). In contrast, the total dipole has a nonzero component in the direction of the surface normal if the incident light is *p*-polarized (electric-field dipole perpendicular to the metal surface). The larger the incident angle, the larger the total electric-field dipole at the metal surface for *p*-polarized radiation. **(b)** If a surface-confined COO^- group is oriented as shown here, then the vibrating dipole for the symmetric stretching vibration, μ_s, will be perpendicular to the metal surface, while the vibrating dipole for the asymmetric stretch vibration, μ_{as}, will be parallel to the metal surface. The surface selection rule dictates that μ_s, but not μ_{as}, will be excited by *p*-polarized radiation.

EXPERIMENTAL

Most of the chemicals used were of the highest purity available from Aldrich Chemical (Milwaukee, WI). 4-Hydroxythiophenol (90%) was further purified by vacuum sublimation. Dimethyloctylchlorosilane was purchased from Hüls America (Somerset, NJ). *Trans*-cinnamic acid was used as received from Eastman Kodak (Rochester, NY). Au substrates were prepared by evaporation of 20–30 nm of Cr or Ti and 200 nm of Au onto polished Si wafers. Self-assembled monolayers of nonylmercaptan ($CH_3(CH_2)_8SH$) and octadecylmercaptan ($CH_3(CH_2)_{17}SH$) were prepared by soaking nominally clean Au substrates in 1.0 mM ethanol solutions of the mercaptans for ~24 h and then rinsing with ethanol and water.

The FTIR-ERS measurements were performed using a Bio-Rad Digilab (Cambridge, MA) FTS-40 spectrometer, which consisted of a water-cooled, 1500 °C ceramic source, a KBr beamsplitter with a 2-in. clear aperture, and a high-sensitivity, 1-mm narrow-band mercury-cadmium-telluride (MCT) detector operating in the 4400–700-cm^{-1} range. A 3-mm source aperture was selected to improve IR beam collimation and polarization. The aperture and reflectance accessory served to attenuate the IR beam to an intensity approaching the maximum linear range of the MCT detector. Enhanced sensitivity was obtained when an optical filter, which passes energies in the 3950–1975-cm^{-1} range, and a larger aperture setting (4 mm) were used.

Spectra were acquired as 256 signal-averaged scans at 2-cm^{-1} resolution and a modulation frequency of 20 kHz, resulting in a measurement time of ~4 min. The signal amplitude was adjusted to take advantage of the effective 19-bit dynamic range of the A/D converter (ADC). The Fourier transformation was performed with one level of zero-filling and boxcar apodization, which provided the highest possible spectral resolution. All spectra were referenced to a freshly prepared Au substrate. A typical measurement obtained for light incident on the substrate at 85° from the surface normal resulted in a noise level of 5×10^{-5} AU.

An N_2-purged glove box, built in our laboratory, was attached to the instrument by magnetic strips and used to isolate the open sample compartment from the laboratory ambient environment. This approach permitted multiple samples to be loaded into the glove box simultaneously, thus eliminating the need for extensive purging of the instrument's sample compartment between spectral acquisitions.

FTIR-ERS spectra were obtained using a Harrick Scientific (Ossining, NY) Seagull reflection accessory equipped with a 1-cm-diameter KRS-5 wire-grid polarizer. The accessory may be configured for experiments involving incident angles spanning the 5°–87° range without the need for optical realign-

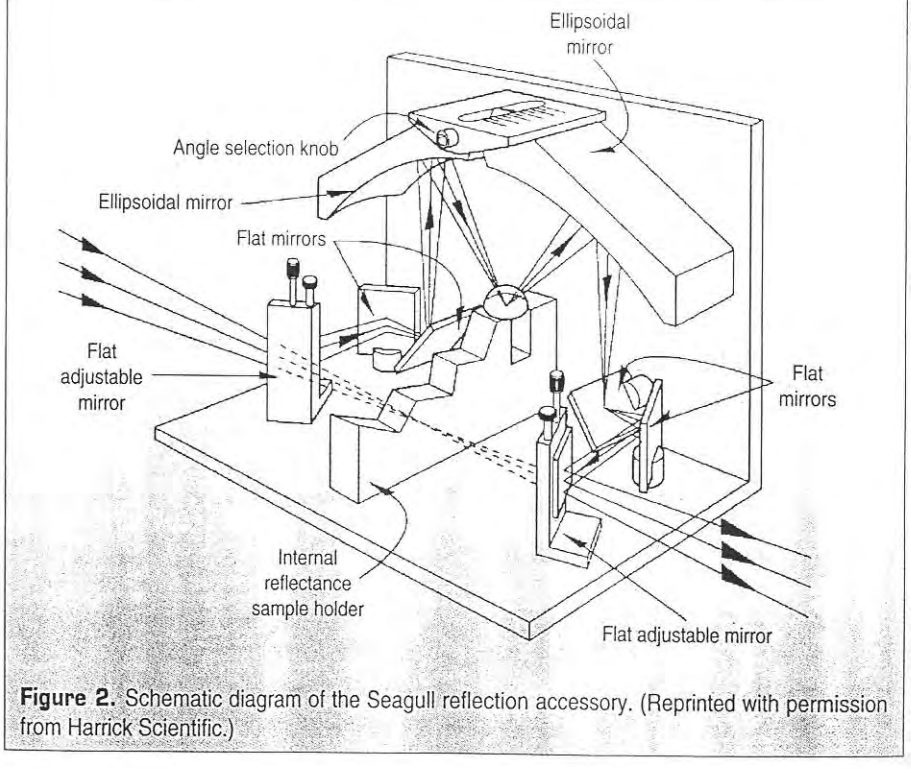

Figure 2. Schematic diagram of the Seagull reflection accessory. (Reprinted with permission from Harrick Scientific.)

ment. This optical design results in no polarization dependence on the angle of incident radiation. A schematic diagram of the Seagull reflectance accessory is shown in Figure 2.

The reaction between surface-confined 4-hydroxythiophenol (4-HTP) and vapor-phase dimethyloctylchlorosilane ($[CH_3(CH_2)_7](CH_3)_2SiCl$), which is discussed in the next section, was studied using a laboratory-built flow cell designed to fit onto the Seagull reflectance accessory (Figure 3a). The flow cell consists of a cover and a base. Two NaCl windows (International Crystal Laboratories, Garfield, NJ) are glued onto the ends of the cell with silicone rubber (Dow Corning, Midland, MI). Flanged Teflon nuts (¼" × 28) of the type used in liquid chromatography connect the cell in series to the Teflon gas-flow lines. The cell base contains a recessed region for the Au/Cr/Si substrate. A silicone O ring is compressed by four mounting nuts to seal the cover to the base. Gas-flow meters control two N_2 streams: One is directed into a vial that contains a solid or liquid reactant with a significant vapor pressure, and the other is used to dilute the first stream to achieve a desired partial pressure of the reactant (Figure 3b). Substrate dosing can be monitored in real time by continuously recording FTIR-ERS spectra: 16 scans and 8 cm^{-1} spectral resolution result in a time resolution of 5 s/spectrum.

Table I. Frequency assignments for octadecylmercaptan (ODM) and nonylmercaptan (NM) (29).

ODM (cm^{-1})	NM (cm^{-1})	Vibrational mode*
2965	2965	CH_3 (C–H asym str)
2937	2938	CH_3 (C–H sym str [FR])
2920	2922	CH_2 (C–H asym str)
2878	2879	CH_3 (C–H sym str [FR])
2851	2852	CH_2 (C–H sym str)

* str = stretch, asym = asymmetric, sym = symmetric, and FR = Fermi resonance.

RESULTS AND DISCUSSION

Introduction to organic monolayer spectroscopy. Spectral characterization of long-chain aliphatic mercaptan monolayer films serves as an illustrative example of FTIR-ERS. A spectrum of the hydrocarbon stretching region for an octadecylmercaptan (ODM) monolayer confined to a Au substrate is shown in Figure 4a. The instrumental baseline response is shown in Figure 4b to illustrate the sensitivity and linearity of the detector response. The band assignments for the ODM monolayer are given in Table I. FTIR-ERS spectra for monolayer films, such as that shown in Figure 4a, contain a very high density of information. Besides the simple assignment of vibrational frequencies, data such as these have revealed that ODM monolayers confined to textured Au surfaces reside in a crystalline or solidlike environment and consist of primarily all-*trans* extended molecular chains that are tilted ~30° from the surface normal as shown in Figure 5 (3).

Typical absorbances for organic monolayer films are on the order of 10^{-3}, and therefore FTIR-ERS requires a high degree of instrument sensitivity and stability as well as measurement repeatability. The measured absorbance intensity may diminish under conditions that enlarge the focal beam and reduce the spectral resolution, polarization efficiency, or the mean angle of the incident light. The unscaled IR signal amplitude for light incident on the substrate at 85° and a 3-mm aperture setting was measured at 4 V, which is 40% of the ADC limit. Hence, FTIR-ERS produces data having a S/N comparable to transmission IR analysis.

Monolayers composed of nonylmercaptan (NM) are more difficult to study by FTIR-ERS because these films are roughly half as thick as the ODM monolayers and are somewhat more structurally disordered. The NM spectrum shown in Figure 6a was obtained using the optical bandpass filter described in the experimental section. The band assignments for these data are given in Table I. Note the improvement in the noise level that results from using the bandpass filter (Figure 6b) compared to the spectrum shown in Figure 4b, which was obtained in the absence of filtering.

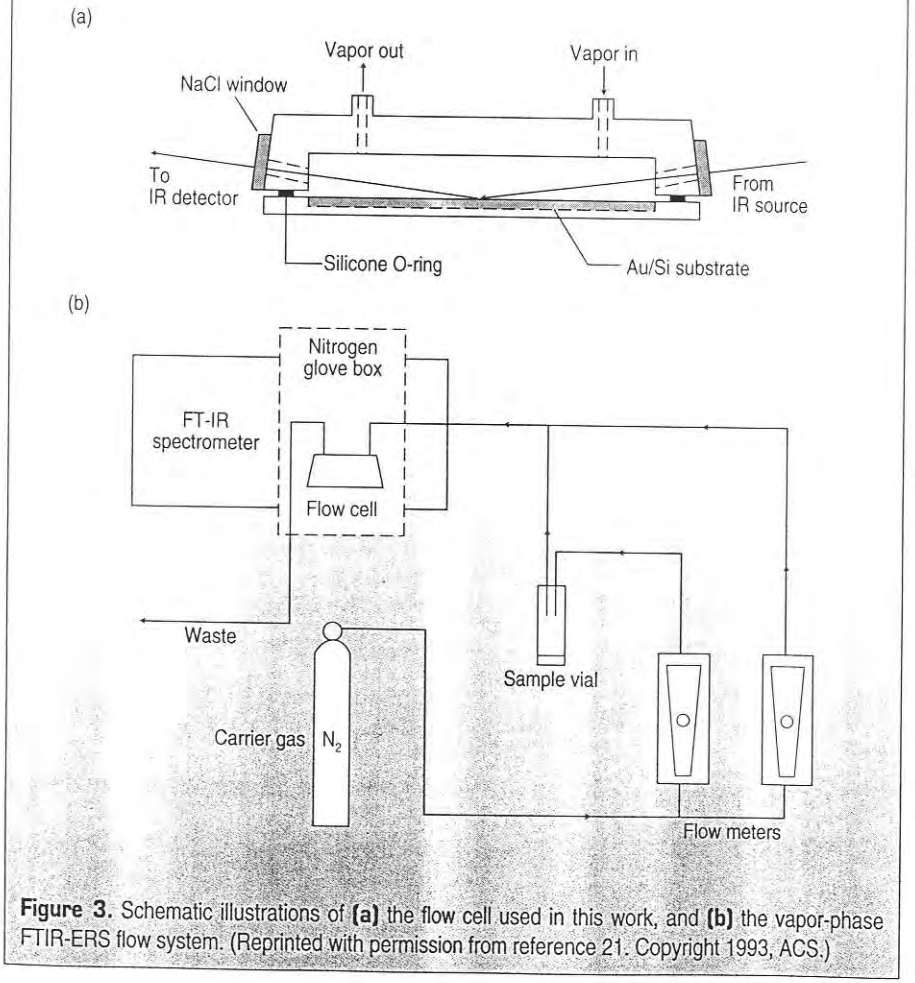

Figure 3. Schematic illustrations of **(a)** the flow cell used in this work, and **(b)** the vapor-phase FTIR-ERS flow system. (Reprinted with permission from reference 21. Copyright 1993, ACS.)

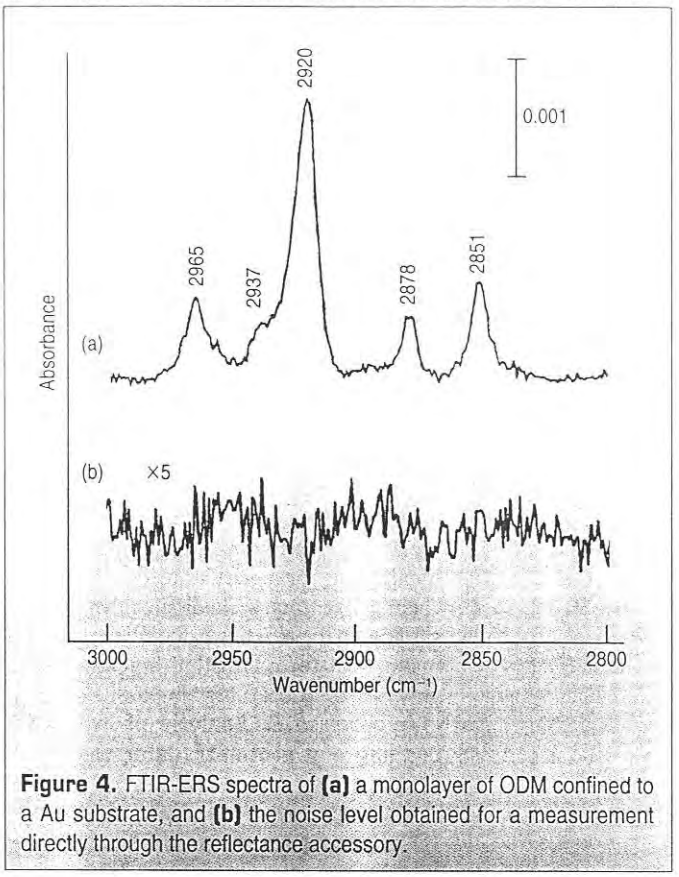

Figure 4. FTIR-ERS spectra of **(a)** a monolayer of ODM confined to a Au substrate, and **(b)** the noise level obtained for a measurement directly through the reflectance accessory.

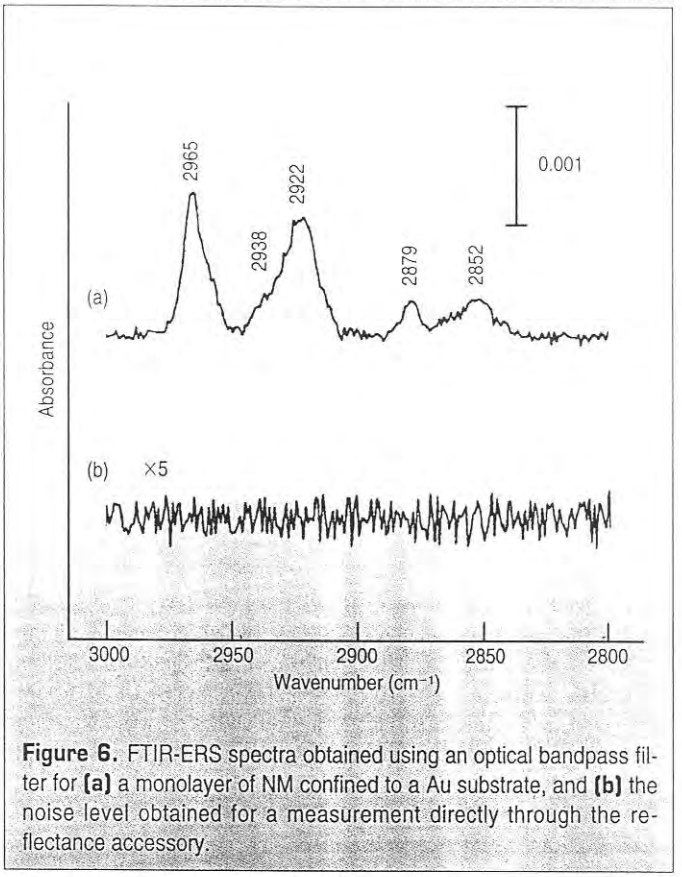

Figure 6. FTIR-ERS spectra obtained using an optical bandpass filter for **(a)** a monolayer of NM confined to a Au substrate, and **(b)** the noise level obtained for a measurement directly through the reflectance accessory.

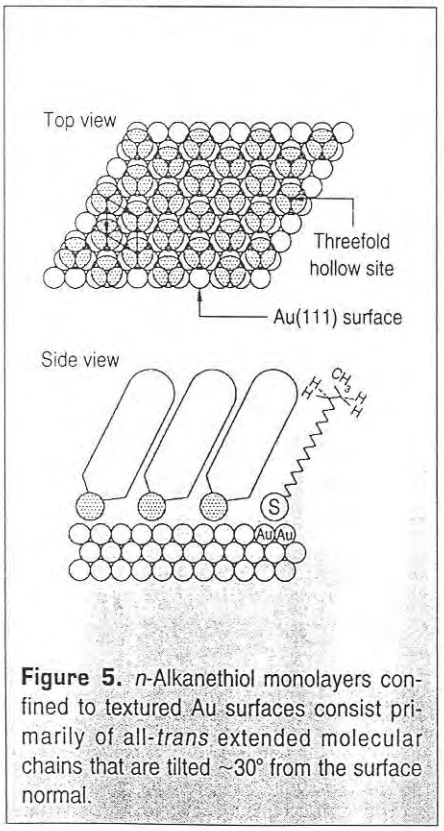

Figure 5. *n*-Alkanethiol monolayers confined to textured Au surfaces consist primarily of all-*trans* extended molecular chains that are tilted ~30° from the surface normal.

APPLICATIONS OF FTIR-ERS TO ORGANIC MONOLAYERS

In this section we examine three recent applications of FTIR-ERS that are relevant to current areas of chemical research. These applications derive from our interest in fundamental aspects of intermolecular interactions between surface-confined, self-assembled monolayers and vapor-phase probe molecules, and chemical sensing applications of these. Interested readers are referred to the original literature for more specific information about the experimental details and spectral interpretation (12, 20–24).

Application 1: In-situ analysis of a chemical reaction between a surface-confined organic monolayer and a vapor-phase reactant. We used in-situ FTIR-ERS to examine the coupling reaction between a surface-confined monolayer of 4-HTP adsorbed on a polycrystalline Au substrate and vapor-phase dimethyloctylchlorosilane (20, 21). The reaction sequence is illustrated in Figure 7, and spectra representing each step are shown in Figure 8.

First, we exposed the naked Au substrate to a pure N_2 purge until a stable background spectrum was obtained. Next, the Au surface was exposed to a 50%-of-saturation $HS(C_6H_4)OH$ vapor stream for 12 min, and the spectrum shown in Figure 8a was obtained. The spectrum shown in Figure 8b was obtained after purging with pure N_2 for 7 min to remove condensed multilayers of the adsorbate (20, 21,24). Next, the Au surface was exposed to a 50%-of-saturation dimethyloctylchlorosilane vapor stream for 12 min (Figure 8c), and finally the flow cell was again purged with pure N_2 for 10 min (Figure 8d).

The peak assignments for the spectra shown in Figure 8b, which correspond to the $Au/HS(C_6H_4)OH$ surface, are as follows: aromatic ring vibrations at 1594, 1579, 1487, and 1428 cm^{-1}; a broad C–O stretching peak at 1264 cm^{-1}; and a broad phenolic O–H stretching peak centered at 3350 cm^{-1} (20,21,25). After introduction of the silane coupling agent and subsequent N_2 purging (Figure 8d), there are important spectral changes. The somewhat enhanced aromatic ring stretches are still present at 1582 and 1485 cm^{-1}, but the phenolic O–H band, originally presented at 3350 cm^{-1} (Figure 8b), has disappeared.

The two overlapping bands at 1277 and 1260 cm^{-1} result from the asymmetric Si–phenoxy stretch and the symmetric H_3C–Si–CH_3 bending mode, respectively (20,21,26,27), and the strong absorptions present between 2850

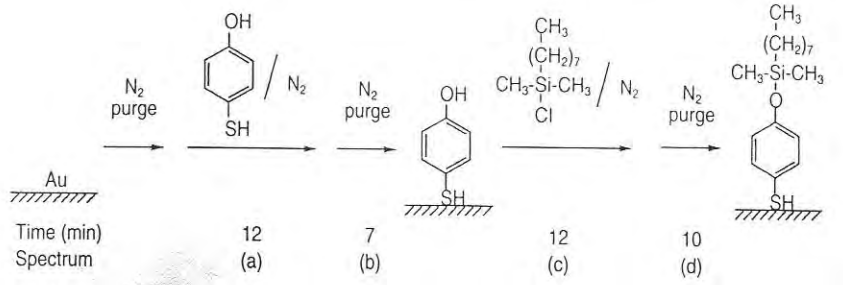

Figure 7: Schematic illustration of the coupling reaction between a surface-confined monolayer of 4-HTP adsorbed on a polycrystalline Au substrate and vapor-phase dimethyloctylchlorosilane. The times and spectrum numbers refer to Figure 8. (Reprinted with permission from reference 21. Copyright 1993, ACS.)

and 2970 cm^{-1} result from the C–H stretching modes of the methyl and methylene groups of the hydrocarbon portion of the coupling agent. More importantly, a new absorption at 918 cm^{-1} (indicated by an asterisk) arises from the symmetric Si–phenoxy stretching mode of the Au/HS(C_6H_5)O–Si(CH_3)$_2$[$CH_3(CH_2)_7$] reaction product (20,21,25–27). Note that the height of this peak is the same in Figures 8c and 8d, even though the intervening N_2 purge greatly attenuates all other absorptions that arise from the coupling agent. The important point is that the band at 918 cm^{-1} is unique to the surface-confined monolayer, and therefore it is possible to measure the kinetics of this surface reaction even in the presence of an ambient-phase reactant (21).

We confirmed the presence of monolayer coverages of the reactant and product using a nanogravimetric surface acoustic wave (SAW) technique (24,28) and optical ellipsometry (20). The results of these experiments corroborate the FTIR-ERS data: precisely stoichiometric coupling occurs between the two reactants to yield a chemically distinct monolayer composed of the two reactants.

These experiments demonstrate the feasibility of changing the chemical properties of surfaces, in this case from hydrophilic to hydrophobic, by means of an in-situ, vapor-phase chemical reaction. Surface transformations such as those described here have important implications for molecular recognition-based chemical sensors, technologies that require surface characteristics to be altered on demand, and for controlled layer-by-layer growth of functional ultrathin films.

Application 2: Analysis of hydrogen-bonding and proton-transfer reactions

between a surface-confined organic monolayer and vapor-phase reactants. Here, we show that surface-confined monolayers of acid-functionalized organomercaptans interact with acidic or basic vapor-phase molecules by hydrogen-bonding interactions or proton-transfer reactions, respectively (22,23). Hydrogen-bonding systems are typified by the interactions of *n*-alkanoic acids ($CH_3(CH_2)_nCOOH$, n = 0–14) with Au surfaces modified by 3-mercaptopropionic acid ($Au/HS(CH_2)_2COOH$), as shown in Figure 9. Such chemical systems can serve as models for natural membrane systems, and they form a basis for molecular recognition chemical sensors.

Figure 10 shows FTIR-ERS data for $Au/HS(CH_2)_2COOH$ and $Au/HS(CH_2)_2CH_3$ surfaces after and before exposure to a saturated vapor of myristic acid, $CH_3(CH_2)_{12}COOH$. Before $CH_3(CH_2)_{12}COOH$ modification, the $Au/HS(CH_2)_2COOH$ spectrum, Figure 10b, indicates absorptions due to the acid C=O stretch and the enhanced α-CH_2 scissors mode at 1722 and 1410 cm^{-1}, respectively (22, 29–32). After dosing, the presence of a second

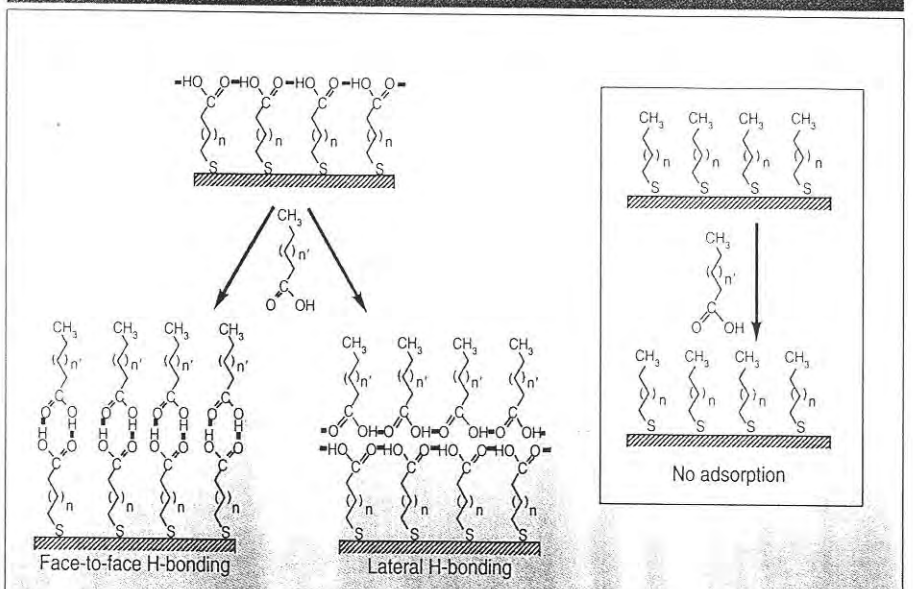

Figure 9. Hydrogen-bonding systems are typified by the interactions of *n*-alkanoic acids with Au surfaces modified with acid-terminated SAMs. (Reprinted with permission from reference 22. Copyright 1992, ACS.)

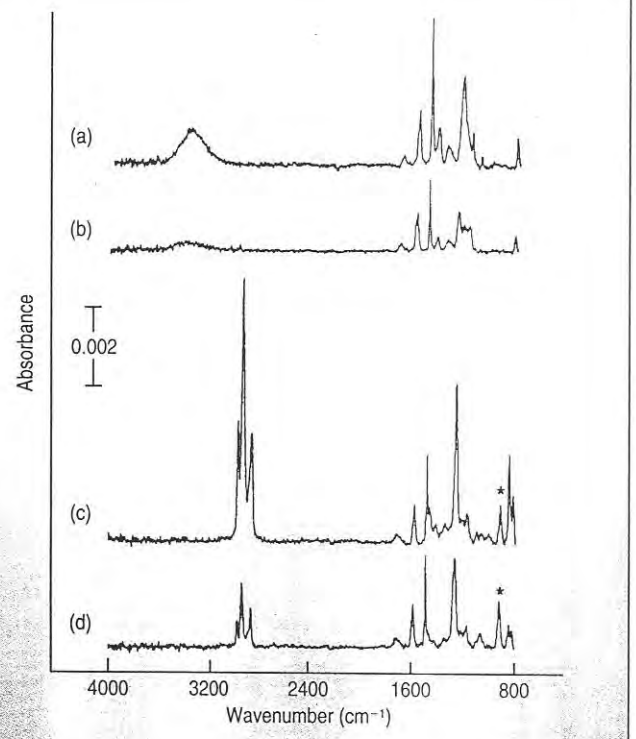

Figure 8. FTIR-ERS spectra arising from a surface-monolayer silane coupling reaction. Each spectrum follows a reaction step, as shown in Figure 7. The band at 918 cm^{-1}, which corresponds to the product of the surface-reaction, is marked with an asterisk. (Reprinted with permission from reference 21. Copyright 1993, ACS.)

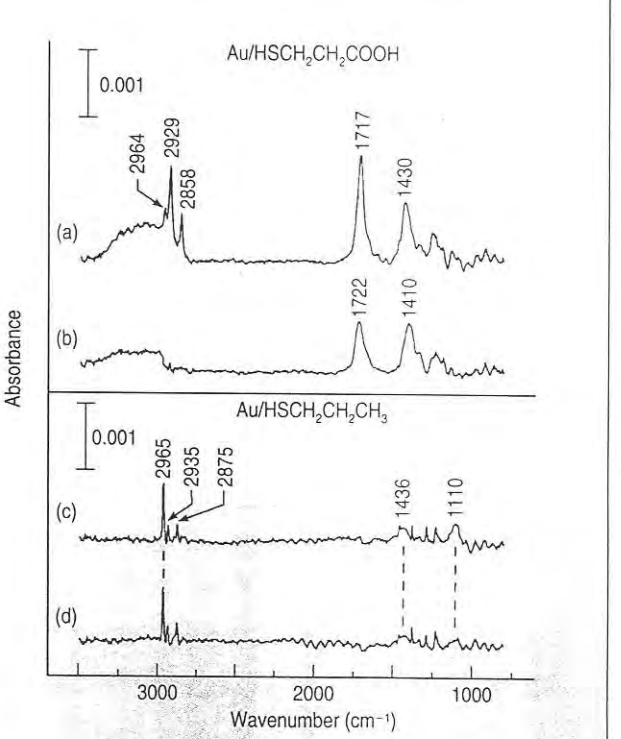

Figure 10. FTIR-ERS spectra of a $Au/HS(CH_2)_2COOH$ surface before **(b)** and after **(a)** exposure to vapor-phase $CH_3(CH_2)_{12}COOH$; and FTIR-ERS spectra of a $Au/HS(CH_2)_2CH_3$ surface before **(d)** and after **(c)** exposure to vapor-phase $CH_3(CH_2)_{12}COOH$. (Reprinted with permission from reference 22. Copyright 1992, ACS.)

surface-confined $CH_3(CH_2)_{12}COOH$ layer is confirmed by the appearance of the methyl C–H stretching vibration at 2964 cm^{-1}, the increased intensity of the methylene C–H stretching vibrations at 2929 and 2858 cm^{-1}, and the doubling of the intensity of the C=O stretching vibration at 1717 cm^{-1} (Figure 10a).

We performed control experiments by exposing a methylated surface to vapor-phase *n*-alkanoic acids as shown on the right side of Figure 9. The FTIR-ERS spectrum of a surface-confined monolayer of $HS(CH_2)_2CH_3$ is shown in Figure 10d. The peak at 2965 cm^{-1} is due to the asymmetric methyl C–H stretching vibration, and the asymmetric and symmetric methylene C–H stretching vibrations are at 2935 and 2875 cm^{-1}, respectively. Other peaks attributable to hydrocarbon backbone modes are present at lower frequencies. The FTIR-ERS spectrum of the methyl-terminated surface after exposure to $CH_3(CH_2)_{12}COOH$ (Figure 10c) is identical to the surface before acid dosing. This result shows that only the acid-surface promotes bilayer formation.

Closer examination of the FTIR-ERS data presented in Figure 10 provides additional evidence for hydrogen bonding between the Au/$HS(CH_2)_2COOH$ and $CH_3(CH_2)_{12}COOH$ layers. The band at 1722 cm^{-1} in Figure 10b has been assigned to the C=O stretching vibration for a laterally hydrogen-bonded carboxylic acid terminal group, as shown in Figure 9 (29,30). After $CH_3(CH_2)_{12}COOH$ exposure, the band shifts to 1717 cm^{-1} (Figure 10a). It has been shown previously that a 16 cm^{-1} shift in the C=O stretching frequency of *n*-alkanoic acids from ~1726 to 1710 cm^{-1} corresponds to a structural change from a face-to-face dimer to a laterally hydrogen-bonded configuration (29,31). Based on the observed frequency shift of 5 cm^{-1}, we propose a model in which adsorbed $CH_3(CH_2)_{12}COOH$ is hydrogen-bonded to Au/$HS(CH_2)_2COOH$ in both face-to-face and lateral configurations, that is, a dynamic superposition of the two configurations shown on the lower portion of Figure 9 (22).

We obtained additional evidence for hydrogen bonding of vapor-phase probe molecules to surface-confined, acid-functionalized mercaptans by using *t*-cinnamic acid (CNMA) as the probe molecule (Figure 11). The C=O stretching vibration for the CNMA face-to-face dimer has an absorption frequency at 1684 cm^{-1} (33). Therefore, a face-to-face hydrogen-bonding interaction between an adsorbed CNMA layer and Au/$HS(CH_2)_2COOH$ will result in a significant shift of the C=O stretching absorption to lower energy. The observed C=O stretching vibration for hydrogen-bonded CNMA on the Au/$HS(CH_2)_2$ COOH surface is 1708 cm^{-1} (Figure 11a). This value is higher than the C=O stretching frequency estimated for the face-to-face Au/$HS(CH_2)_2COOH$/CNMA dimer, 1696 cm^{-1} (34), but lower than the frequency observed for the Au/$HS(CH_2)_2COOH$/$HOOC(CH_2)_{12}CH_3$ bilayer. This result suggests that both face-to-face and lateral hydrogen-bonding configurations are present, consistent with our earlier conclusion.

Figure 12 presents FTIR-ERS spectra for a Au/$HS(CH_2)_{10}COOH$ monolayer before and after exposure to a saturated vapor of $CH_3(CH_2)_9NH_2$. Before amine exposure (Figure 12b), the asymmetric and symmetric C–H stretching vibrations, which result from the methylene groups in the Au/$HS(CH_2)_{10}COOH$ monolayer, are present at 2919 and 2849 cm^{-1}, respectively. The bands at 1739 and 1718 cm^{-1} are due to the C=O stretching vibrations of nonhydrogen-bonded and laterally hydrogen-bonded COOH terminal groups, respectively, as discussed earlier. The absence of a high-energy O–H stretching band is consistent with prior studies of acids in solid-state-like environments (25,29), and the effect may be compounded in the present case by the surface-IR selection rule.

After the COOH-terminated monolayer surface is exposed to $CH_3(CH_2)_9NH_2$ vapor, a layer of $CH_3(CH_2)_9NH_2$ adsorbs, as indicated in Figure 12a by the increased intensity of the methylene stretching bands at 2921 and 2853 cm^{-1}, and the appearance of the asymmetric and symmetric methyl vibrations at 2966 and 2879 cm^{-1}, respectively. Importantly, the C=O band at 1739 cm^{-1} (Figure 12b), which corresponds to nonhydrogen-bonded COOH groups, disappears after amine exposure, whereas most of the C=O band intensity at 1718 cm^{-1}, which corresponds to laterally hy-

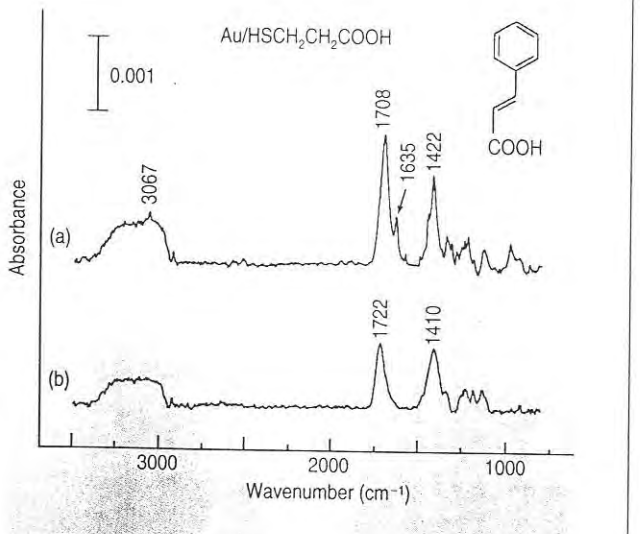

Figure 11. FTIR-ERS spectra of a Au/$HS(CH_2)_2COOH$ surface before **(b)** and after **(a)** exposure to vapor-phase CNMA. The structure of CNMA is shown in the upper right corner of the figure. (Reprinted with permission from reference 22. Copyright 1992, ACS.)

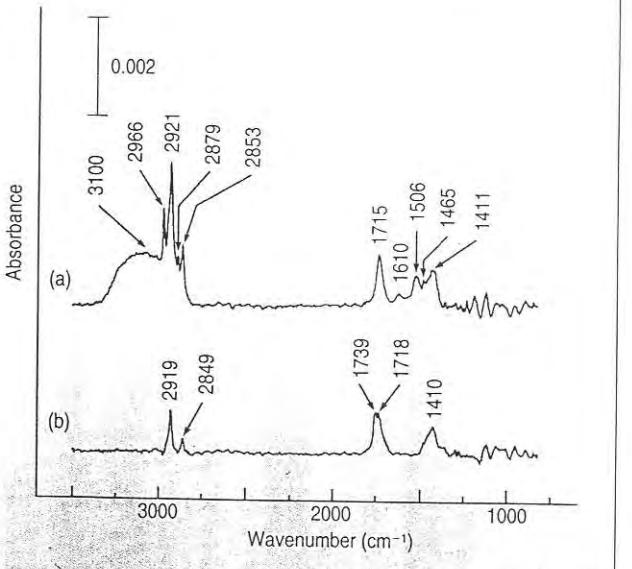

Figure 12. FTIR-ERS spectra of a Au/$HS(CH_2)_{10}COOH$ monolayer before **(b)** and after **(a)** exposure to vapor-phase $CH_3(CH_2)_9NH_2$. (Reprinted with permission from reference 21. Copyright 1993, ACS.)

drogen-bonded COOH groups, remains and shifts slightly to 1715 cm^{-1}. We assign the band at 1506 cm^{-1} (Figure 12a) to the N–H symmetric bending mode of the NH_3^+ groups, which are formed by the vapor-phase acid–base reaction between COOH and NH_2 groups (25). The N–H asymmetric bending mode corresponding to NH_3^+ groups is not observed, at least partially as a result of an orientation effect. If we assume that the alkane chains are perpendicular to the plane of the substrate surface, then their asymmetric bending dipoles will be parallel to the surface and thus inaccessible for surface IR excitation. The new band centered at 3100 cm^{-1}, which is broadened by intramonolayer hydrogen bonding, corresponds to the N–H stretching modes of NH_3^+ (25). The band at 1610 cm^{-1} is assigned to the asymmetric stretching vibration of COO^- (25).

The bands at 1465 and 1411 cm^{-1} are difficult to assign with certainty, and the assignments given here should be viewed with caution. The 1411 cm^{-1} band probably corresponds to the α-CH_2 bending (scissors) mode, and the band at 1465 cm^{-1} may arise from either an enhancement of the remaining CH_2 scissors modes or the COO^- symmetric stretching mode, or a superposition of both (25,29). The FTIR-ERS spectrum shown in Figure 12a does not exhibit noticeable change for at least 10 h, indicating that the bilayer structure formed after amine exposure is quite stable. This result is in contrast to the hydrogen-bonded bilayers, which are stable for much shorter periods.

Application 3: A chemically sensitive monolayer coating for sensor applications. In this application we discuss a chemically sensitive monolayer coating that selectively binds organophosphonates. We have constructed and tested a SAW-based chemical sensor that utilizes the composite monolayer, and this section illustrates how FTIR-ERS permitted us to verify the structure of the monolayer and its selective chemical interaction with the nerve-gas simulant diisopropylmethylphosphonate (DIMP) (12).

Chemical sensors usually consist of a chemically sensitive coating supported by a chemically inert physical transducer (28). Because the exact nature of the intermolecular interactions between the coating and the target analyte are often ambiguous, the design of selective sensor coatings is based largely on trial and error. A more appealing approach to sensor fabrication relies upon a rational design based on known, bulk-phase interactions between the analyte and the selective coating. FTIR-ERS is very well suited for correlating surface and bulk-phase interactions.

The coating design discussed in this section takes advantage of the interaction between organophosphonate nerve-agent simulants and a composite monolayer consisting of Cu^{2+} tethered to a Au substrate by an ordered, carboxylate-terminated *n*-alkanethiol monolayer. The rationale for this design is that Cu^{2+} and some of its chelates are hydrolysis catalysts for certain nerve agents (35). Thus, a surface layer of coordinatively unsaturated Cu^{2+} might be expected to provide selective and reversible binding sites for organophosphonates. The general approach is illustrated in Figure 13, where the analyte (**D**) represents a DIMP molecule.

The formation of a carboxylate/Cu^{2+}-terminated monolayer, such as that illustrated in Figure 13, was confirmed by FTIR-ERS. Figure 14a shows the FTIR-ERS spectrum for a monolayer of the protonated form of mercaptoundecanoic acid (MUA) before Cu^{2+} adsorption. The asymmetric and symmetric methylene stretching frequencies at 2925 and 2854 cm^{-1}, respectively, are typical for a

monolayer of acid-terminated *n*-alkanethiols (22,23,29,30). The two bands centered around 1440 cm^{-1} were discussed previously. Peaks due to the C=O stretching mode at 1740 and 1717 cm^{-1} indicate that the acid groups are protonated and present as a mixture of free monomers and laterally hydrogen-bonded dimers or short oligomers, respectively (29, 31,32).

We obtained the spectrum shown in Figure 14b after the acid-terminated surface was immersed in a dilute Cu^{2+}/EtOH solution for a few minutes. The methylene stretching region is essentially identical to that shown in Figure 14a, but significant changes are apparent in the C=O stretching region. The two carbonyl stretching bands at 1740 and 1717 cm^{-1} have disappeared, and a new absorbance, which represents the asymmetric C–O stretch of the carboxylate groups, is present at about 1609 cm^{-1}. There are also some changes in bands near 1450 cm^{-1}, but this region is somewhat difficult to interpret, and readers are referred to the specialty literature for a detailed analysis (23,25,29). The peak at 1609 cm^{-1} strongly suggests that the surface has been deprotonated and is complexed to Cu^{2+} (25,30). XPS data, which are not shown here, also confirm the presence of approximately monolayer coverage of Cu^{2+} (12).

Figure 14c shows the difference spectrum obtained by subtracting Figure 14b from a spectrum recorded 2–5 min after ex-situ dosing of the composite monolayer with a DIMP/N_2 vapor for 20 min. Several peaks characteristic of DIMP are present: the P–O stretch at 1016 cm^{-1}; the hydrogen-bonded P=O stretch at 1206 cm^{-1}; the symmetric bending mode of the P-bound CH_3 groups at 1315 cm^{-1}; the resonance-split symmetric bending mode of the isopropyl methyl groups at 1385 cm^{-1}; and the asymmetric C–H stretch of the isopropyl methyl groups at 2984 cm^{-1} (12,25). The frequencies and magnitudes of the peaks in Figure 14c conclusively demonstrate that *under these conditions* approximately one monolayer of DIMP adsorbs onto the carboxylate/Cu^{2+} surface.

SAW experiments, which are not discussed here (12), indicate that the selective coating responds proportionally and reversibly to DIMP in a manner readily distinguishable from its response to common organic solvents and water. They also indicate that the sensor is both sensitive and durable. In accord with SAW experiments, the DIMP-related peaks in Figure 14c disappear after ~1 h, which indicates reversible DIMP adsorption (12).

CONCLUSIONS

The results presented in this article show that single-reflection FTIR-ERS can be implemented with excellent S/N for unambiguous analysis of nanometer-thick coatings. S/N can be further improved through the use of a suitable optical filter to limit the intensity of the transmitted radiation only to the spectral regions of particular interest.

We have shown how FTIR-ERS can be used to study intermolecular interactions between molecules in surface-confined organic monolayers and between monolayers and vapor-phase probe molecules. Studies such as these are important from a fundamental perspective, but they also have applications in membrane science, materials chemistry, tribology, and chemical sensing. We have used other techniques, such as ellipsometry, electrochemistry, XPS, and those based on acoustic wave devices to study organic monolayers, but we have found that FTIR-ERS generally provides a higher density of useful chemical in-

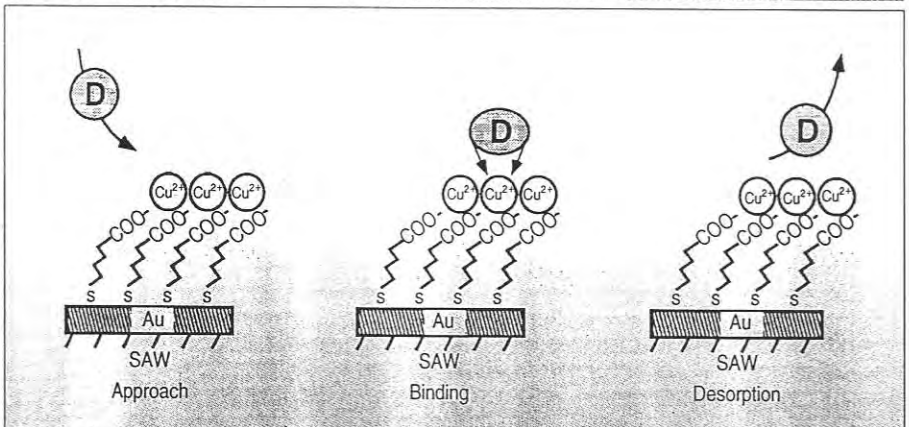

Figure 13. A surface layer of coordinatively unsaturated Cu^{2+} might be expected to provide selective and reversible binding sites for organophosphonates. The analyte (**D**) represents a DIMP molecule. (Reprinted with permission from reference 12. Copyright 1992, ACS.)

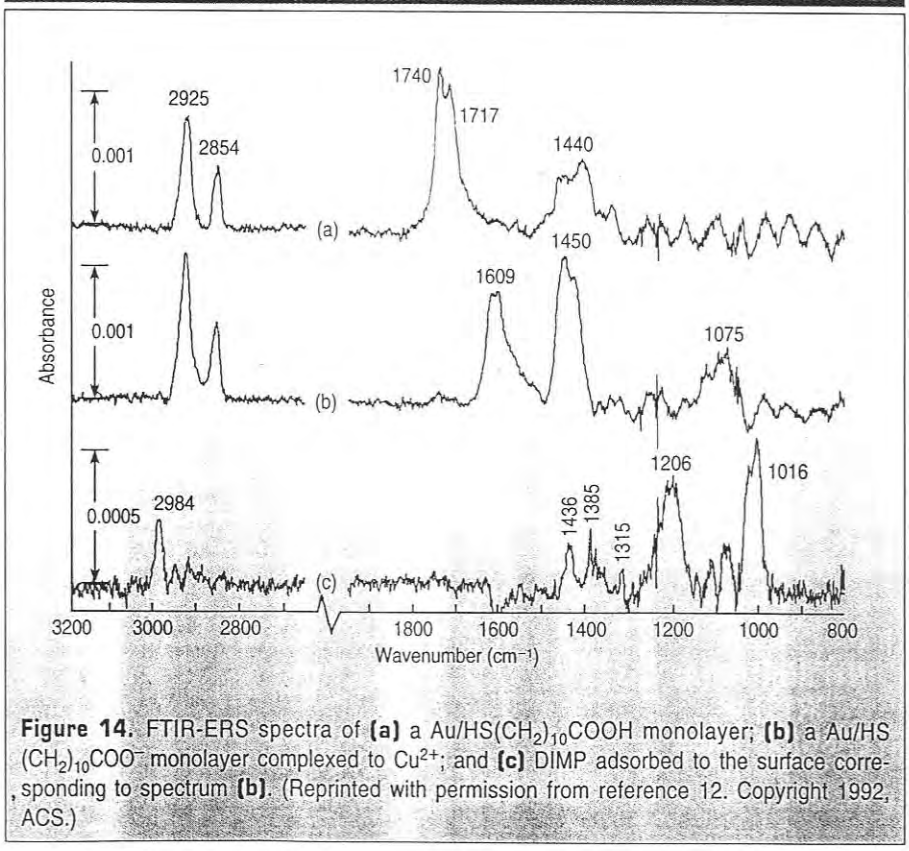

Figure 14. FTIR-ERS spectra of **(a)** a Au/HS$(CH_2)_{10}$COOH monolayer; **(b)** a Au/HS$(CH_2)_{10}COO^-$ monolayer complexed to Cu^{2+}; and **(c)** DIMP adsorbed to the surface corresponding to spectrum **(b)**. (Reprinted with permission from reference 12. Copyright 1992, ACS.)

formation than these other complementary methods.

We believe that there are many differences between two-dimensional and bulk-phase reaction chemistry and that FTIR-ERS will frequently be employed to elucidate these differences in the future.

ACKNOWLEDGMENTS

The authors would like to thank Dr. Larry J. Kepley and Mr. Ross Thomas for helpful discussions. The National Science Foundation (CHE-90146566) and the U.S. Department of Energy (Contract Number DE-AC04-76DP00789) supported this work.

REFERENCES

(1) D.L. Allara and J.D. Swalen, *J. Phys. Chem.* **86,** 2700 (1982).
(2) R.C. Thomas, J.E. Houston, T.A. Michalske, and R.M. Crooks, *Science* **259,** 1883 (1993).
(3) L.H. Dubois and R.G. Nuzzo, *Ann. Rev. Phys. Chem.* **43,** 437 (1992), and references therein.
(4) M.-C. Pham, S.A. Aeiyach, J. Moslih, P. Soubiran, and P.-C. Lacaze, *J. Electroanal. Chem.* **277,** 327 (1990).
(5) D.B. Parry and J.M. Harris, *Appl. Spectrosc.* **42,** 997 (1988).
(6) N.J. Harrick, *Internal Reflection Spectroscopy* (John Wiley & Sons, New York, 1967).
(7) Y.-L. Chen and J.N. Israelachvili, *J. Phys. Chem.* **96,** 7752 (1992).
(8) V. DePalma and N. Tillman, *Langmuir* **5,** 868 (1989).
(9) C.D. Bain and G.M. Whitesides, *Science* **240,** 62 (1988).
(10) C.E.D. Chidsey, *Science* **251,** 919 (1991).
(11) C.B. Ross, L. Sun, and R.M. Crooks, *Langmuir* **9,** 2101 (1993).
(12) L.J. Kepley, R.M. Crooks, and A.J. Ricco, *Anal. Chem.* **64,** 3191 (1992).
(13) A. Kumar, H.A. Biebuyck, N.L. Abbott, and G.M. Whitesides, *J. Am. Chem. Soc.* **114,** 9188 (1992).
(14) K.L. Prime and G.M. Whitesides, *Science* **252,** 1164 (1991).
(15) J.D. Swalen and J.F. Rabolt, *Fourier Transform Infrared Spectroscopy Application to Chemical Systems,* J.R. Ferraro and L.J. Basile, eds. (Vol. 4, Academic Press, Orlando, FL, 1985), p. 283.
(16) S.A. Francis and A.H. Ellison, *J. Opt. Soc. Am.* **49,** 131 (1959).
(17) N.J. Harrick, *Am. Lab.* **18,** 78 (1986).
(18) M.D. Porter, *Anal. Chem.* **60,** 1143A (1988).
(19) B.J. Barner, M.J. Green, E.I. Saez, and R.M. Corn, *Anal. Chem.* **63,** 55 (1991).
(20) L. Sun, R.C. Thomas, R.M. Crooks, and A.J. Ricco, *J. Am. Chem. Soc.* **113,** 8550 (1991).
(21) C. Xu, L. Sun, L.J. Kepley, R.M. Crooks, and A.J. Ricco, *Anal. Chem.* **65,** 2102 (1993).
(22) L. Sun, L.J. Kepley and R.M. Crooks, *Langmuir* **8,** 2101 (1992).
(23) L. Sun, R.M. Crooks, and A.J. Ricco, *Langmuir* **9,** 1775 (1993).
(24) R.C. Thomas, L. Sun, R.M. Crooks, and A.J. Ricco, *Langmuir* **7,** 620 (1991).
(25) L.J. Bellamy, *The Infrared Spectra of Complex Molecules* (3rd Ed., Chapman and Hall, London, 1975).
(26) D.R. Anderson, *Analysis of Silicones,* A.L. Smith, ed. (John Wiley & Sons, New York, 1974), Chapter 10.
(27) The band assignments for surface-confined $HS(C_6H_4)OSi(CH_3)_2[(CH_2)_7CH_3]$ have been confirmed by comparison to an authentic sample of $(C_6H_5)OSi(CH_3)_2[(CH_2)_7CH_3]$. See Reference 20.
(28) R.C. Hughes, A.J. Ricco, M.A. Butler, and S.J. Martin, *Science* **254,** 74 (1991).
(29) R.G. Nuzzo, L.H. Dubois, and D.L. Allara, *J. Am. Chem. Soc.* **112,** 558 (1991).
(30) A. Ihs and B.J. Liedberg, *J. Coll. Interface Sci.* **144,** 282 (1991).
(31) J. Yarwood, *Spectroscopy* **5**(6), 34 (1990).
(32) C.E.D. Chidsey and D.N. Loiacono, *Langmuir* **6,** 682 (1990).
(33) *The Aldrich Library of FT-IR Spectra,* 1st Ed., C.J. Pouchert, ed. (Vol. 2, Aldrich Chemical Co., Milwaukee, WI, 1985), p. 174.
(34) The C=O stretching frequency for the mixed face-to-face $HS(CH_2)_2COOH/CNMA$ dimer is estimated by averaging the C=O stretching frequencies for a face-to-face $HS(CH_2)_2COOH$ dimer (1708 cm^{-1}) and a face-to-face CNMA dimer (1684 cm^{-1}).
(35) T. Wagner-Jauregg, B.E. Hackley, Jr., T.A. Lies, O.O. Owens, and R. Proper, *J. Am. Chem. Soc.* **77,** 922 (1955).

Richard M. Crooks *is an associate professor of chemistry at Texas A&M University. At the time of this work he was an assistant professor at the University of New Mexico. He received his PhD in electrochemistry at the University of Texas, Austin. His research interests include the synthesis and characterization of functional, self-assembling organic monolayers, chemical sensors, electrochemical synthesis of nonoxide ceramics, and scanning probe microscopy and lithography.*

Chuanjing Xu *received his PhD in analytical chemistry from the University of Illinois in Urbana. He is now a postdoctoral associate at Texas A&M University studying monolayer reaction chemistry and novel monolayer-based chemical sensors.*

Li Sun *is an assistant professor of chemistry at the University of Minnesota in Minneapolis. He was a postdoctoral associate at the University of New Mexico at the time of this work. He received his PhD from Northwestern University in Evanston, Illinois. His current research interests include self-assembly chemistry, surface-enhanced Raman spectroscopy, and scanning probe microscopy.*

Stephen L. Hill *is a senior applications chemist at the West Coast office of the Digilab Division of Bio-Rad Laboratories. He joined Digilab, Inc., in 1976, following undergraduate studies at the Massachusetts Institute of Technology. His current research interests include infrared microscopy, dichroic polariza-*

tion studies of complex materials, and automated spectroscopic spatial analysis.

Antonio J. Ricco *is a senior member of the technical staff in the microsensor R&D department at Sandia National Laboratories. He received his PhD in inorganic chemistry from MIT in 1984. His research interests focus on solid-state chemical microsensors including SAW devices, optical fibers and waveguides, and silicon-based microelectronic devices.* ♦

Received for peer review 6/7/93.
Revised version accepted 7/6/93.

Call for Papers

Spectroscopy welcomes the opportunity to consider manuscripts for publication that describe the practical application of spectroscopic techniques. For a copy of our guidelines for authors, to discuss a proposed topic, or to submit a completed manuscript, please call, fax, or write:

Linda Crabtree, Editor
Spectroscopy
P.O. Box 10460
Eugene, OR 97440-2460
tel: (503) 343-1200
fax: (503) 344-3514